

The potential of harakeke fibre as reinforcement in polymer matrix composites including modelling of long harakeke fibre composite strength

Tan Minh Le ^{1,2*} and Kim Louise Pickering ¹

¹ School of Engineering, University of Waikato, Gate 8, Hillcrest Road, Hamilton, New Zealand

² Department of Textile Technology, Hanoi University of Science and Technology, Dai Co Viet Street, Hanoi, Vietnam

* Corresponding author

Phone: +64223271411

Fax: +6478384835

Email: tml14@students.waikato.ac.nz

Permanent address: Department of Textile Technology, Hanoi University of Science and Technology, Dai Co Viet Street, Hanoi, Vietnam

ABSTRACT

Mechanical properties of aligned long harakeke fibre reinforced epoxy with different fibre contents were evaluated. Addition of fibre was found to enhance tensile properties of epoxy; tensile strength and Young's modulus increased with increasing content of harakeke fibre up to 223 MPa at a fibre content of 55wt% and 17 GPa at a fibre content of 63wt%, respectively. The flexural strength and flexural modulus increased to a maximum of 223 MPa and 14 GPa, respectively, as the fibre content increased up to 49wt% with no further increase with increased fibre content. The Rule of Mixtures based model for estimating tensile strength of aligned long fibre composites was also developed assuming composite failure occurred as a consequence of the fracture of the lowest failure strain fibres taking account porosity of composites. The model was shown to have good accuracy for predicting the strength of aligned long natural fibre composites.

Keywords: A. Fibres; B. Polymer-matrix composites (PMCs); C. Mechanical properties; D; Modelling; E. Harakeke.

1. Introduction

The use of natural fibres as reinforcement in polymer matrix composites to replace synthetic fibres is currently increasing because of growing environmental awareness, high specific properties and their advantages over synthetic fibres such as low cost, low density, and abundant availability. Research has shown that in certain composite applications, natural fibres have performance comparative with glass fibre, the dominant fibre used in composites [1].

Harakeke is the Maori name for the New Zealand native plant (Fig. 1a) commonly known as New Zealand flax or *Phormium tenax*. However, in this context, the name “flax” is actually a misnomer because harakeke is not biologically related to European flax [2]. Long fibre bundles (Fig. 1b) extracted from harakeke leaves has a long history of use for production of clothes, sacking and rope. In the early 1920s, harakeke products accounted for around 20% of the total export income of New Zealand [2]. However, sales decreased during the 20th century due to the presence of synthetic fibres and the expansion of the sisal industry, and the current use of harakeke is largely confined to crafts [3]. Harakeke fibre is considered to have similar properties to sisal – another leaf fibre [2, 3] which has widely been used as a reinforcement of polymeric composites [4]. Hence, harakeke fibre would be expected to have potential to reinforce polymers.

In this work, the physical and mechanical properties of harakeke fibre were assessed. The tensile and flexural properties of aligned long harakeke reinforced epoxy composites with various fibre volume fractions were also evaluated and modelling was developed for predicting tensile strength of aligned long harakeke-epoxy composites.

2. Experimental

2.1. Materials

Harakeke fibre was obtained from the Templeton Flax Mill, Riverton, New Zealand. Fibre bundles were combed manually in a single direction before being cut to the same length as that of compression mould, and then dried at 80°C overnight before composite fabrication. The matrix was a low viscosity epoxy system comprised of Nuplex resin R180 and Nuplex standard hardener H180 (mixing ratio 5:1 by weight).

2.2 Methods

2.2.1. Density measurement

Natural fibre density can be measured by one of five methods: (1) diameter and linear density, (2) Archimedes, (3) helium pycnometry, (4) gradient column and (5) liquid pycnometry. From these, Archimedes using canola oil as an immersion fluid was adopted here because it is simple, quick to give the test results and bears the lowest cost [5].

Testing was based on ASTM D3800-99 (Standard Test Method for Density of High-Modulus Fibers) using the apparatus as shown in Fig. 2. Three specimens of harakeke fibre bundles weighing about 1 g were oven dried at 60° C for 72 hours and then placed in a vacuum oven at room temperature for 5 minutes to remove trapped air between fibre cells before testing. The average density was calculated.

The density measurement of cured epoxy resin and composites was based on ASTM 792-00 (Standard Test Methods for Density and Specific Gravity (Relative Density) of Plastics by Displacement). Distilled water was used as an immersion fluid. Densities of five cured epoxy and composite specimens were measured and average density was obtained.

2.2.2. Single fibre tensile testing

Single fibre tensile testing was based on ASTM C 1557-03 (Standard Test Method for Tensile Strength and Young's Modulus of Fibers). Thirty elementary (single) fibres were separated from their bundles and mounted on 2 mm thick cardboard with a 2 mm length window that set the fibre gauge length as shown in Fig. 3. The two ends of each fibre were glued to the cardboard using a cyanoacrylate glue. Mounted fibres were observed using an Olympus BX60F5 microscope to make sure they were single. Harakeke single fibre has polygonal cross section [6], but, for simplicity, it was assumed perfectly circular. Diameters of selected fibres were measured at 3 points along the fibre length under the same microscope with a magnification of 200 and the average diameter was calculated and used for calculation of tensile properties. The cardboard windows with a mounted fibre were then individually placed in the grips of an Instron 4204 tensile testing machine fitted with a 10 N-load cell, and the supporting sides of the cards were carefully cut using a hot wire cutter. The fibres were tensile tested to failure at a rate of 0.5 mm/min.

Average fibre tensile strength and Young's modulus and failure strain were obtained using the results from thirty specimens.

Fibres with small diameter do not allow the attachment of an extensometer for measuring the displacement (elongation) of the fibre so fibre elongation can only be measured from the cross-head displacement of the tensile tester. However, the cross-head displacement is the combination of the fibre elongation as well as cross-head, specimen gripping system and specimen mounting card deformation. Therefore, it is necessary to determine the system compliance (C_s) for correcting the fibre elongation. The system compliance was determined experimentally using the guide from the standard ASTM C 1557-03.

The cross-head displacement ΔL (mm) can be expressed by:

$$\Delta L/F = (1/EA)l_o + C_s \quad (1)$$

Where, l_o is the specimen gauge length (mm), E is the Young's modulus of the fibre (MPa), A is the cross-sectional area of the fibre (mm^2) and F is the applied force (N). Therefore, the plot of $\Delta L/F$ (which can be determined from the force versus cross-head displacement curve of the fibre) versus l_o will yield a straight line with slope of $1/EA$ and intercept C_s which is the value of system compliance.

The actual fibre elongation Δl (mm) can be determined by:

$$\Delta l = \Delta L - C_s F \quad (2)$$

And the fibre strain will be:

$$\epsilon = \Delta l/l_o \quad (3)$$

The fibre stress σ (MPa) is expressed by:

$$\sigma = F_{max}/A \quad (4)$$

Where, F_{max} is the maximum applied force (N). The Eq. (2), (3) and (4) were utilised with digital data recorded during tensile testing to produce the actual stress versus strain curve of each specimen. The Young's modulus was determined from the slope of the linear section of the curve. The failure strain was the strain corresponding to maximum force.

2.2.3 Determining lumen volume fraction

Harakeke fibre bundles were granulated to lengths of less than 4 mm and pulped using a laboratory scale digester to remove unwanted components and to break down fibre bundles into single fibres. A mixture of fibre (70 g) and 5%NaOH/2%Na₂SO₄ solution with ratio of 1:8 by weight were heated in a closed stainless steel canister from ambient temperature to 170°C over 90 min and then held at 170°C for 40 minutes. The pulp was cooled and thoroughly washed with water, then dried in an oven at 80°C for 48 hours. These pulped fibres (single fibres) were used to determine single fibre diameter and fibre wall thickness using a Kajaani Fibrelab electronic sequential fibre analyser. Approximately 6000 fibres were analysed and a mean fibre diameter and fibre wall thickness were determined. Assuming that fibre lumen and single fibre cross sections are circular and consistent along the fibre length, lumen diameter would be:

$$D_l = D_f - 2T_w \quad (5)$$

where D_l , D_f and T_w are lumen diameter, fibre diameter and fibre wall thickness, respectively and

lumen volume fraction in single fibres would be:

$$V_l = v_l/v_{sf} = A_l/A_{sf} \quad (6)$$

and

lumen volume fraction in fibre bundles would be:

$$V'_l = v_l/v_{fb} \quad (7)$$

where v is volume and A is cross sectional area; subscripts l , sf and fb denotes lumen, single fibre and fibre bundle, respectively.

Combination of (6) and (7) leads to:

$$V'_l = V_l(v_{sf}/v_{fb}) = V_l(m_{sf}/m_{fb})(\rho_{fb}/\rho_{sf}) \quad (8)$$

where:

$$Y_p = m_{sf}/m_{fb} \quad (9)$$

and Y_p is the pulp yield; m_{sf} and m_{fb} are the mass of oven-dried single fibres (pulped fibres) and fibre bundles, respectively; ρ is density.

Fibre bundles were considered to be completely separated into single fibres after digesting. Pulped fibres were not long enough for density determination so their density was assumed to be the same as the fibre bundle density obtained as described in Section 2.2.1. Therefore, Eq. 8 would become:

$$V'_l = V_l Y_p \quad (10)$$

Composite porosity due to fibre lumen is:

$$P_l = V'_l V_f \quad (11)$$

where V_f is fibre volume fraction in composites

2.2.3. Composite manufacture

The fabrication of harakeke/epoxy composites was similar to that which has been used to make European flax/epoxy composites [7]. Combed and dried continuous fibre bundles (Fig. 1c) were hand laid into a simple rectangular mould (size: 22 x 15 x 0.3 cm), which had been lined by a Teflon sheet, to form a fibre mat. Composites with six different nominal fibre contents (15, 25, 35, 45, 55 and 65 wt%) were produced. The epoxy resin and hardener were thoroughly mixed in a plastic cup and then degassed in a vacuum oven at room temperature for 10 minutes. The epoxy mixture was poured over the fibre mat and a wide flat ended metal scraper was used to spread resin over the mat and squeeze trapped air out. The resin impregnated fibre mat was left for resin to soak into the mat for 20 minutes before being degassed in a vacuum environment for 5 minutes to remove trapped air. A steel plate was then laid on the top of the mould. Finally, the mould was placed into a compression moulder and then the epoxy soaked fibre mat was pressed until the mould closed and was left for curing for 24 hours. Due to resin coming out from the mould during pressing fibre content was calculated based on weight of fibre and composites. The composite sheet was removed from the mould and post cured for 4 hours in an oven at 80°C.

2.2.4 Composite tensile testing

Composite tensile testing was based on ASTM D 3039 (Standard Test Method for Tensile Properties of Polymer Matrix Composite Materials) using abrasive paper tabs within the grips. Six composite specimens with nominal dimensions of 200 x 15 x 3 mm were cut from cured composite sheets using a circular saw. Specimens were then polished with abrasive paper. The tensile properties of neat epoxy were measured according to ASTM D 638 - 03 (Standard Test Method for Tensile Properties of Plastics). Six dumbbell-shaped epoxy specimens were cast and

cured in a silicone mould for 24 hours and then post cured at 80°C in an oven for 4 hours. All tensile specimens were conditioned at 23° ± 3° C and 50% ± 5% relative humidity for 40 hours and then tested on an Instron-4204 universal testing machine fitted with a 50 kN load cell at a crosshead speed of 5 mm/min. Strain was measured using an Instron 2630-112 extensometer with a 50 mm gauge length. The mean value of tensile strength and Young's modulus of composites and neat epoxy were calculated.

2.2.5. Composite flexural testing

Cured composites were cut into six flexural test specimens with nominal dimension of 85 x 12.7 x 3 mm using a circular saw. Specimens were then polished with abrasive paper. The flexural test (three-point bending) was carried out in accordance with ASTM D 790-03 (Standard Test Methods for Flexural Properties of Unreinforced and Reinforced Plastics and Electrical Insulating Materials) on an Instron-4204 fitted with a 5 kN load cell. A support span-to-depth ratio of 16:1 and a crosshead speed of 2 mm/min were used. The average flexural strength and flexural modulus were calculated.

2.2.6. Microscopy

An optical light microscope Olympus BX60F5 was used to determine if fibres are single and measure fibre diameter for single fibre tensile testing. A WILD M3B stereo microscope fitted with a Nikon camera (Digital Sight DS-U1) was used to study composite sample surfaces after flexural. Fibre surfaces and tensile fracture surfaces of composites were investigated using a Hitachi S4100 field emission scanning electron microscope (FESEM) operated at 5 kV. All samples were mounted on aluminium stubs using carbon tape and then sputter coated with platinum to make them conductive prior to observation.

3. Results and discussion

3.1 Fibre morphology

In harakeke leaves, fibre bundles have different cross sectional shapes including “key-holes” and “horseshoes” or “molar teeth” [6, 8-11]. The “key-hole” bundles which have larger cross section are located in the upper part of the leaf while the “horseshoe” bundles are in the lower part and between these bundles, in the centre of the leaf are helical fibril cells with a thin wall called vascular bundles which are considered to be the pathways of fluids in the

leaf [9, 10]. The fibre bundles are usually surrounded by thin walled cells known as sheath cells and cuticles or epidermis still adhere to the fibre bundles at the side close to the leaf surface [6, 10]. When fibre bundles are extracted from the leaves, some of them are longitudinally split into smaller bundles [10]. Fig. 4 shows examples of all the above features of harakeke fibre. “Key-hole” and “horseshoe” bundles and fragmented bundles are shown in Fig. 4a and vascular bundles, sheath cells and cuticles are labelled v, s and c respectively. Fig. 4b shows the helical structure of vascular bundles. The surface of a harakeke fibre bundle is shown in Fig. 4c. It can be seen that the surface is uneven with ridges along the length of the fibre which may enhance mechanical bonding between fibre bundles and the matrix. However, non-cellulose compounds such as waxes or fats and surface impurities known to be present on such untreated fibre may limit bonding at the interface between fibre bundles and the polymeric matrix [9]. Harakeke long fibre bundles extracted from the harakeke plant leaves contain single fibres (also called individual / elementary fibres / ultimate fibres). The single fibre has a polygonal cross-section with a central lumen surrounding by a thick wall and the length of elementary fibre varies from 3.7-5.2 mm and the diameter is approximately 10 – 15 μm [6, 12, 13]. In this work, a diameter of 14.98 μm and cell wall thickness of 2.72 μm were found from data on Kajaani Fibrelab. Therefore, lumen diameter using Eq. 5 would be 9.54 μm . A single fibre and its lumen were assumed perfectly circular so the area fraction of fibre wall thickness cross-section would be equal to $1 - (D_l/D_f)^2 = 0.59$. This figure was used to correct the tensile strength and Young’s modulus by dividing tested values of harakeke fibre by a corrected factor of 0.59. This manner of correcting tensile strength and Young’s modulus for harakeke fibre has been reported in the literature [8]. The fibre lumen fraction which was calculated based on fibre lumen diameter, cell wall thickness, single fibre diameter and fibre pulp yield (that was found to be 0.53) using Eq. 6 and 10 is presented in Table 1. Harakeke lumen fraction was similar to sisal and jute but significantly higher than other natural fibres. The high lumen fraction of harakeke fibres was expected to significantly contribute to harakeke composite porosity.

3.2 Physical and mechanical properties of harakeke fibres

The system compliance of the tensile testing system was determined using Eq. (1) with gauge lengths of single harakeke fibres of 2, 3 and 4 mm using the graph shown in Fig. 5. Comparison of the best fit equation $y = 0.462x + 0.3136$ to Eq. (1), where y is $\Delta L/F$ and x is gauge length gives the value of the system compliance $C_s = 0.3136$ as the

intercept with the y-axis. This value was applied to correct the fibre elongation and produce stress-strain curves for each specimen, an example of which is shown in Fig. 6. It can be seen that the stress-strain curves of the fibres moved to the left on applying the system compliance such that failure strain would reduce and Young's modulus would increase relative to uncorrected values. A typical stress-strain graph for harakeke fibre (see Fig. 6) had an initial non-linear portion which was attributed to the orientation of the fibrils along the axis of the fibre under load [14]. With higher loading, the fibre response became linear and this linear was used for Young's modulus determination using a linear regression equation fitted to the data. The average Young's modulus, tensile strength and failure strain as well as density of fibres are reported in Table 2 with the values in the brackets being standard deviation. This is the first time the density of harakeke fibre has been directly measured and reported as far as the authors are aware. It can be seen that harakeke density (1.27 g/cm^3) is significantly lower than other fibres while the tensile strength (778 MPa) and Young's modulus (32.09 GPa) are comparable to others. This suggests that harakeke fibre could contribute to higher specific mechanical properties of composites. In Fig. 7, the tensile strength values of harakeke individual fibres were plotted as a function of their diameter. It shows a decrease of tensile strength as diameter increases. This trend has been reported for other natural fibres [15-18]. The wide scatter of tensile values is a typical drawback of natural fibres which can result in variability of composite properties.

3.3 Composite tensile properties

Average tensile strength and Young's modulus of composite specimens with different fibre weight fractions and cured epoxy specimens are presented in Figs. 8 and 9, respectively. These figures show that the addition of harakeke fibre makes epoxy stronger and stiffer even at a fibre content as low as 13wt% with an increase of 71% and 82% for the tensile strength and Young's modulus, respectively. Tensile strength and Young's modulus can be seen to share the same trend of increase with fibre volume fraction up to a fibre content of 55wt%. At a fibre content of 55wt%, the average tensile strength and Young's modulus of harakeke fibre composites were 223 MPa and 16.8 GPa, which are 4.6 fold and 4.3 fold higher than those of neat epoxy, respectively. These figures compare well with the results of 211 MPa and 14.7 GPa for tensile strength and Young's modulus, respectively, reported in the literature on harakeke-epoxy composites at the same fibre volume fraction [6]. However, as fibre content

increased to 63wt%, tensile strength of harakeke fibre decreased to 193 MPa, although Young's modulus increased modestly to 17.2 GPa. It could be explained that at this high fibre content, the wetting of fibre by epoxy became worse resulting in weaker fibre/matrix bonding which caused the reduction of composite tensile strength.

However, with fibre bonding not being so important to Young's modulus, this still increased further with higher fibre content.

Table 3 shows the absolute and specific tensile properties of harakeke based composites compared to glass and other cellulose based fibre reinforced epoxy composites with the same fibre configuration (long aligned fibre). It can be seen that tensile strength and Young's modulus of harakeke fibre composites are lower than those of glass fibre composite but the difference between specific Young's moduli is small; 15.6 GPa.g/cm³ for harakeke fibre composites compared to 18 GPa.g/cm³ for glass fibre composites. The tensile strength of harakeke fibre composites (223 ± 14 MPa) is greater than that of sisal fibre composites (211 ± 12MPa) but the Young's modulus of sisal fibre composites is higher, 19.7 ± 1.5 GPa, compared to 16.8 ± 0.62 GPa.

3.4 Composite flexural properties

Micrographs of composites after flexural testing are shown in Fig. 10. It appears that composite samples did not fail after the test but micro crack happened on the tension surface. Average flexural strength and flexural modulus of aligned long harakeke reinforced epoxy composites with different fibre contents are presented in Figs. 11 and 12, respectively, for the first time. It can be seen that the flexural strength and flexural modulus of harakeke/epoxy composites increases as the fibre content increases up to 49wt%; at this fibre content, the flexural strength and flexural modulus of composites are 223MPa and 13.7 GPa. Further addition of harakeke fibre did not bring about improvement of these flexural properties. The trend is similar to that for pulped harakeke fibre reinforced epoxy reported in the literature [19] with fibre content up to 50wt%. However, in this research, flexural properties at higher fibre contents were not investigated so their trend above 50wt% was not reported. The maximum flexural strength and modulus of about 190 MPa and 9.5 GPa, respectively, were found at fibre content of about 50wt% which are lower than the figures found in our work.

3.5 Modelling of tensile properties of long aligned harakeke fibre composites

3.5.1 Calculation of fibre volume fraction and porosity

Fibre and matrix volume fraction were calculated using the equations [20]:

$$V_f = W_f(\rho_c/\rho_f) \quad (12)$$

$$V_m = 1 - V_f - V_p \quad (13)$$

where V, W and ρ are volume fraction, weight fraction and density, respectively; subscripts f, m, p and c denotes fibre, matrix, porosity and composite, respectively.

Total porosity of composites was calculated using the equation [21]:

$$V_p = (\rho_{ct} - \rho_c)/\rho_{ct} \quad (14)$$

where:

$$\rho_{ct} = \rho_f V_f + \rho_m V_m \quad (15)$$

such as ρ_{ct} is theoretical density of composites.

Values of fibre volume fraction, matrix volume fraction, total porosity and lumen porosity (using Eq. 11) are presented in Table 4. Significant porosity is typical for natural fibre composites, but has largely been ignored in modelling. However Madsen et al have taken account of porosity relating to processing (matrix porosity and that at fibre/matrix interface) although due to fibre collapse in their work, lumens were not considered to contribute to this [22, 23]. However, for the harakeke composites investigated in the present work, fibre lumens did not collapse (see Fig. 13) and contributed significantly to composite porosity (Table 4) due to the large lumen fraction in fibre bundles (Table 1). It is appreciated that the values of lumen porosity were obtained based on the assumption that the density of single fibre was the same as that of the fibre bundles, however, given the value of 1.27 g/cm³ for fibre bundle density and the maximum possible value for single fibres being that for pure crystallised cellulose of 1.5 g/cm³ [24], this reflects a maximum possible reduction of 15% for lumen porosity and therefore, the lumen porosity can still be considered to be the major component of porosity. However, this assumption did not affect the total porosity which was calculated from theoretical and actual composite densities and total porosity would be

used in modelling discussed later. The total porosity was assumed to be a variable function of the fibre weight fraction [22]. For simplicity, the total porosity fraction was modelled as a linear function (see Fig. 14) using data in Table 4:

$$V_p = 0.2742W_f - 0.0063 \quad (16)$$

3.5.2 Young's modulus

Young's modulus of aligned long harakeke composites (E_c) may be predicted using the Rule of Mixtures considering the effect of composite porosity [22, 23]:

$$E_c = (E_f V_f + E_m V_m)(1 - V_p)^2 \quad (17)$$

where E is Young's modulus and V_p was substituted from Eq. 16. Note that, Young's modulus applied in the modelling was corrected by dividing the value in Table 2 by 0.59 (see Section 3.1). Results of Young's modulus predictions are presented in the Fig. 15. The predicted Young's moduli are 13 - 29% higher than experimental ones with prediction depending on fibre volume fractions.

3.5.3 Tensile strength

The composite strength (σ_c) may be estimated using the Rule of Mixtures including porosity as follows [22]:

$$\sigma_c = (\sigma_f V_f + \sigma_m V_m)(1 - V_p)^2 \quad (18)$$

where σ_f and σ_m is fibre strength and matrix strength, respectively. This equation assumes a perfect interface which, given epoxy as a matrix, would appear to be a reasonable assumption. Corrected average tensile strength of the fibre and tested average tensile strength of the matrix were substituted into the Eq. 20 and the predicted and experimental strengths perfect interface of the composites are shown in Table 5. The predicted values are larger than the experimental ones from 135% to 243% depending on fibre volume fraction.

Due to the large gap between predicted and experimental tensile strengths of the composites, an alternative model for predicting the tensile strength of the aligned long fibre composites was considered. It can be seen that the average fibre and epoxy matrix failure strains are 4.54% (Table 2) and 2.91% (Table 3), respectively, which at first sight does not explain composites failing at a lower average strain of about 1.44%. However, due to the variability

of natural fibre properties, some fibres would have failed at strains lower than their average failure strain; fibre failure strain varied significantly with standard deviation of 2.35% equivalent to a coefficient of variation of 36.3%. Therefore, it was assumed that composite failure could be initiated when fibres with the lowest failure strain failed giving a lowest fibre failure strain based Rule of Mixtures model expressed by:

$$\sigma_c = (\sigma^*_f \cdot V_f + \sigma^*_m \cdot V_m) \cdot (1 - V_p)^2 \quad (19)$$

where now σ^*_f and σ^*_m are the fibre stress and matrix stress at the failure strain of the weakest fibres. These values were taken as the average stresses of all the tested fibres and epoxy samples, respectively, at the lowest failure strain of all the single fibres which was estimated from the distribution of fibre failure strains (Fig. 16). Probability, P_f , was calculated using an estimator commonly used in application of the Weibull distribution:

$$P_f = (j - 0.5)/n \quad (20)$$

where n is the number of data points and j is the rank of the j -th data point

A cubic regression function was found to best fit the data. The lowest failure strain of 1.41% was found at the point that the probability was equal to 0. The stress on each tested fibre at the strain of 1.41% was obtained using the corrected stress-strain curves as mentioned previously (an example in Fig. 6). The average stress of all fibre specimens (σ_f) at strain of 1.41% was 401 MPa (ignoring the lumen) and the average stress of all epoxy samples was 35.5 MPa. Note that, the corrected fibre stress of 680 MPa (464/0.59) was substituted into Eq. 19 to estimate tensile strength of aligned long harakeke/epoxy composites. The predicted and experimental strengths are presented in Fig. 16. The prediction error varied from 5 to 24 % which is much improved from the Rule of Mixtures just taking account of porosity. It is possible that some of this difference could be accounted for by less than perfect interfacial bonding.

Normally, the prediction error for Young's modulus and tensile strength of natural fibre composites using the conventional Rules of Mixtures increases at higher fibre volume fraction, but it did not happen to harakeke composites investigated in this work using the model taking account of porosity, supporting that the porosity

significantly affects the mechanical properties of aligned long harakeke composites, especially at high fibre volume fractions.

4. Conclusions

The addition of aligned long harakeke fibre was found to significantly enhance the tensile and flexural properties of epoxy. The tensile properties, which were comparable to those of other cellulose based fibre composites, show the potential of harakeke fibre used in composites. Lumen volume in harakeke fibre is significant and must be considered to calculate tensile strength and Young's modulus of fibre and porosity of the composites. The model developed for predicting composite strength based on composites assumed to fail when fibres with the lowest failure strains failed and considering the effect of porosity could be used to predict the tensile strength of aligned long harakeke fibre (or similar fibres) composites.

Acknowledgements: The author would like to thank Vietnamese Government Scholarship Fund for granting the scholarship.

References

1. Hu, R. and J.-K. Lim, *Fabrication and mechanical properties of completely biodegradable hemp fiber reinforced polylactic acid composites*. Journal of Composite Materials, 2007. **41**(13): p. 1655-1669.
2. Duchemin, B. and M. Staiger, *Treatment of Harakeke fiber for biocomposites*. Journal of Applied Polymer Science, 2009. **112**(5): p. 2710-2715.
3. Newman, R., et al., *Epoxy composites reinforced with deacetylated Phormium tenax leaf fibres*. Composites Part A, 2007. **38**(10): p. 2164-2170.
4. Li, Y., Y. Mai, and L. Ye, *Sisal fibre and its composites: a review of recent developments*. Composites Science and Technology, 2000. **60**(11): p. 2037-2055.
5. Ma, X., J. Yu, and J.F. Kennedy, *Studies on the properties of natural fibers-reinforced thermoplastic starch composites*. Carbohydrate Polymers, 2005. **62**(1): p. 19-24.
6. Newman, R., et al., *Failure mechanisms in composites reinforced with unidirectional Phormium leaf fibre*. Composites Part A, 2009.
7. Andersons, J., E. Spārniņš, and R. Joffe, *Stiffness and strength of flax fiber/polymer matrix composites*. Polymer Composites, 2006. **27**(2): p. 221-229.
8. King, M.J. and J.F. Vincent, *Static and dynamic fracture properties of the leaf of New Zealand flax Phormium tenax (Phormiaceae: Monocotyledones)*. Proceedings of the Royal Society of London. Series B: Biological Sciences, 1996. **263**(1370): p. 521-527.
9. De Rosa, I., C. Santulli, and F. Sarasini, *Mechanical and thermal characterization of epoxy composites reinforced with random and quasi-unidirectional untreated Phormium tenax leaf fibers*. Materials and Design, 2009.
10. King, M., *Phormium tenax (Agavaceae) leaf anatomy effects on fibre extraction by the Maori haro method*. New Zealand Journal of Botany, 2003. **41**(3): p. 571-578.
11. Cruthers, N., et al., *Methods for characterizing plant fibers*. Microscopy research and technique, 2005. **67**(5): p. 260-264.
12. Cruthers, N.M., et al., *Structural differences among fibers from six cultivars of Harakeke (Phormium tenax, New Zealand flax)*. Textile research journal, 2006. **76**(8): p. 601-606.
13. Carr, D., et al., *Fibers from three cultivars of New Zealand flax (Phormium tenax)*. Textile research journal, 2005. **75**(2): p. 93-98.
14. Andersons, J., et al., *Strength distribution of elementary flax fibres*. Composites Science and Technology, 2005. **65**(3): p. 693-702.
15. De Rosa, I.M., et al., *Morphological, thermal and mechanical characterization of okra (< i> Abelmoschus esculentus</i>) fibres as potential reinforcement in polymer composites*. Composites Science and Technology, 2010. **70**(1): p. 116-122.
16. Bodros, E. and C. Baley, *Study of the tensile properties of stinging nettle fibres (< i> Urtica dioica</i>)*. Materials Letters, 2008. **62**(14): p. 2143-2145.
17. Shibata, M., et al., *Biodegradable polyester composites reinforced with short abaca fiber*. Journal of Applied Polymer Science, 2002. **85**(1): p. 129-138.
18. De Rosa, I.M., et al., *Tensile behavior of New Zealand flax (Phormium tenax) fibers*. Journal of Reinforced Plastics and Composites, 2010. **29**(23): p. 3450-3454.
19. Le Guen MJ and Newman RH, *Pulped Phormium tenax leaf fibres as reinforcement for epoxy composites*. Composites Part A, 2007. **38**(10): p. 2109-2115.
20. Matthews, F.L. and R.D. Rawlings, *Composite materials: engineering and science* 1999: Elsevier.
21. ASTM D2734, *Standard Test Methods for Void Content of Reinforced Plastics*, 2003.

22. Madsen, B. and H. Lilholt, *Physical and mechanical properties of unidirectional plant fibre composites—an evaluation of the influence of porosity*. Composites Science and Technology, 2003. **63**(9): p. 1265-1272.
23. Madsen, B., A. Thygesen, and H. Lilholt, *Plant fibre composites—porosity and stiffness*. Composites Science and Technology, 2009. **69**(7): p. 1057-1069.
24. Sun, C., *True density of microcrystalline cellulose*. Journal of pharmaceutical sciences, 2005. **94**(10): p. 2132-2134.
25. Charlet, K., et al., *Scattering of morphological and mechanical properties of flax fibres*. Industrial Crops and Products, 2010. **32**(3): p. 220-224.
26. Fidelis, M.E.A., et al., *The effect of fiber morphology on the tensile strength of natural fibers*. Journal of Materials Research and Technology, 2013. **2**(2): p. 149-157.
27. Mohanty, A., M. Misra, and G. Hinrichsen, *Biofibers, biodegradable polymers and biocomposites: an overview*. Macromolecular materials and Engineering, 2000. **276**(1): p. 1-24.
28. Oksman, K., et al., *Morphology and mechanical properties of unidirectional sisal-epoxy composites*. Journal of Applied Polymer Science, 2002. **84**(13): p. 2358-2365.
29. Islam, M.S., K.L. Pickering, and N.J. Foreman, *Influence of alkali fiber treatment and fiber processing on the mechanical properties of hemp/epoxy composites*. Journal of Applied Polymer Science, 2011. **119**(6): p. 3696-3707.
30. Van de Weyenberg, I., et al., *Influence of processing and chemical treatment of flax fibres on their composites*. Composites Science and Technology, 2003. **63**(9): p. 1241-1246.
31. Oksman, K., *High quality flax fibre composites manufactured by the resin transfer moulding process*. Journal of Reinforced Plastics and Composites, 2001. **20**(7): p. 621-627.





Fig.1.Harakeke macrographs showing (a) harakeke plant, (b) harakeke fibre bundles and (c) aligned harakeke fibre mat

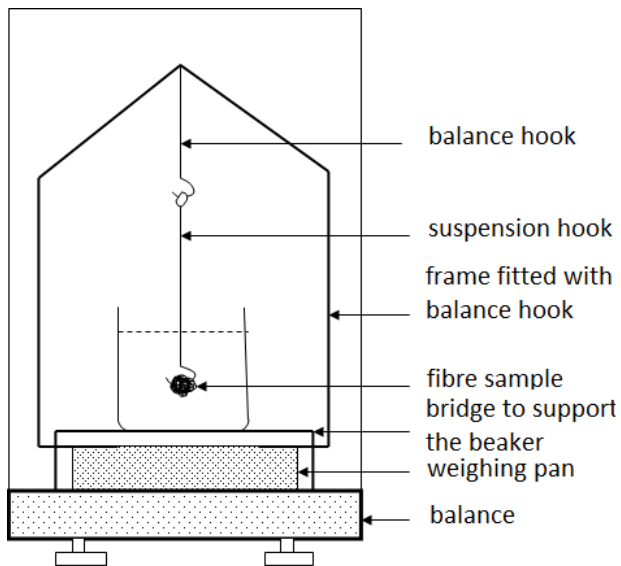


Fig. 2. Schematic diagram of apparatus for density measurement

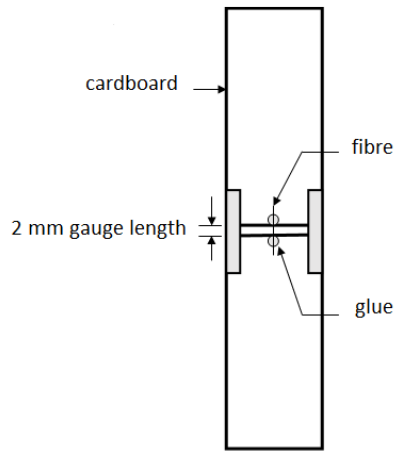


Fig. 3. Schematic diagram of cardboard with a mounted single fibre used in single fibre testing

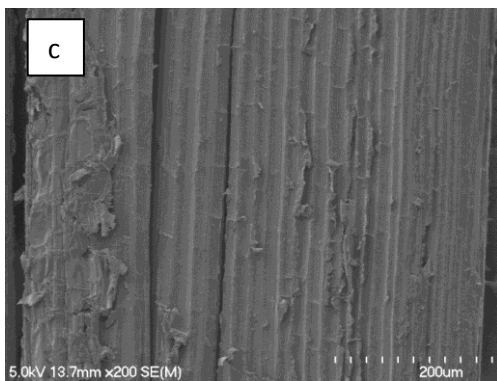
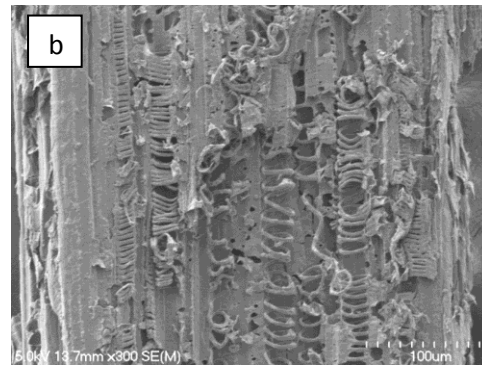
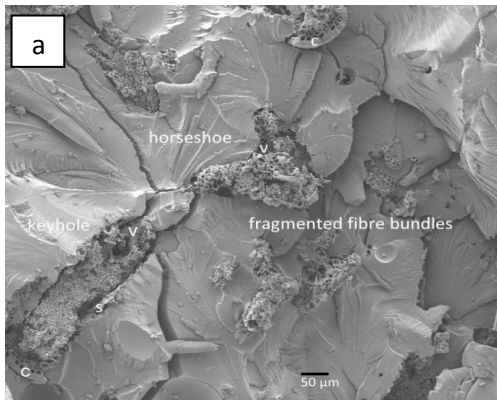


Fig. 4. FESEM images of harakeke fibre morphology: (a) different cross sectional shapes of fibre bundles in composites, (b) helical structure of vascular bundles seen on split as-supplied fibre bundles and (c) fibre bundle surface(as supplied)

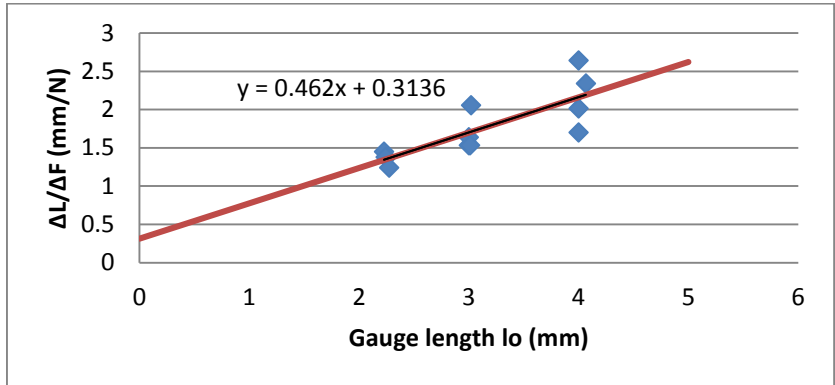


Fig. 5. Graph based on Eq. 1 to obtain system compliance of the tensile testing system

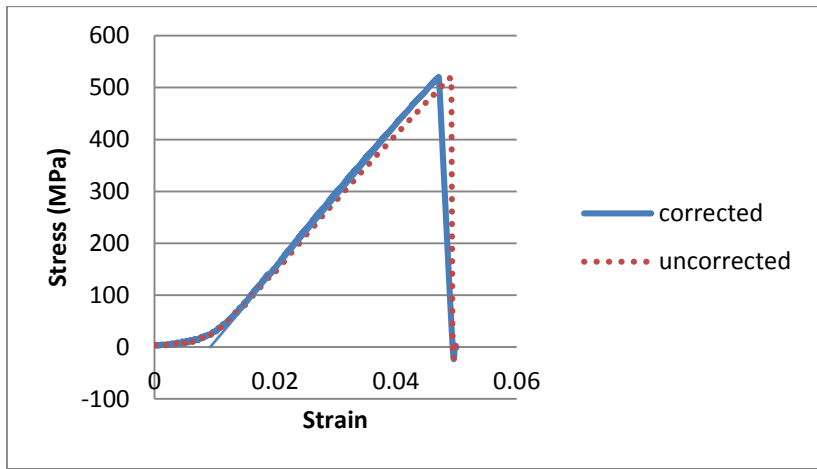


Fig. 6. Typical stress vs strain curves of harakeke fibre uncorrected based on crosshead motion and corrected using C_s

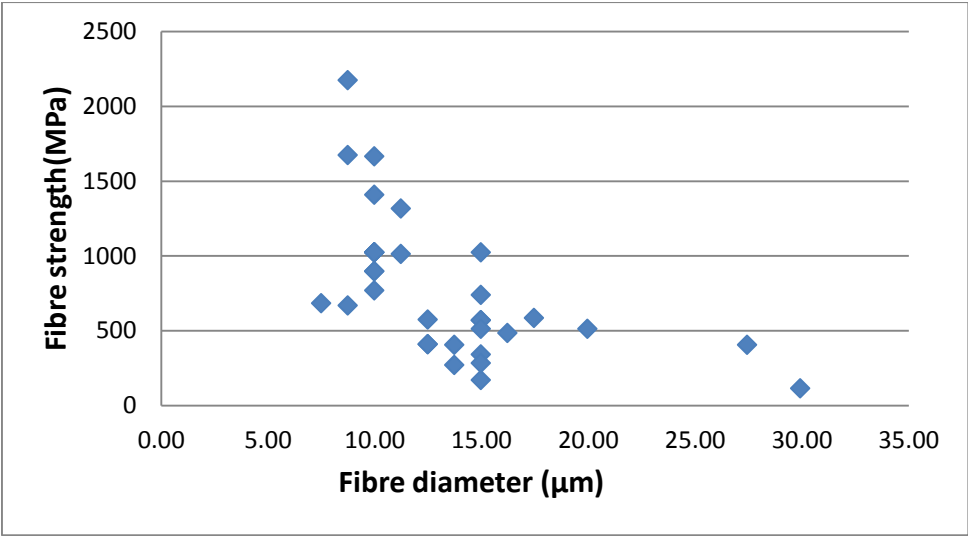


Fig. 7. Single fibre strength versus fibre diameter

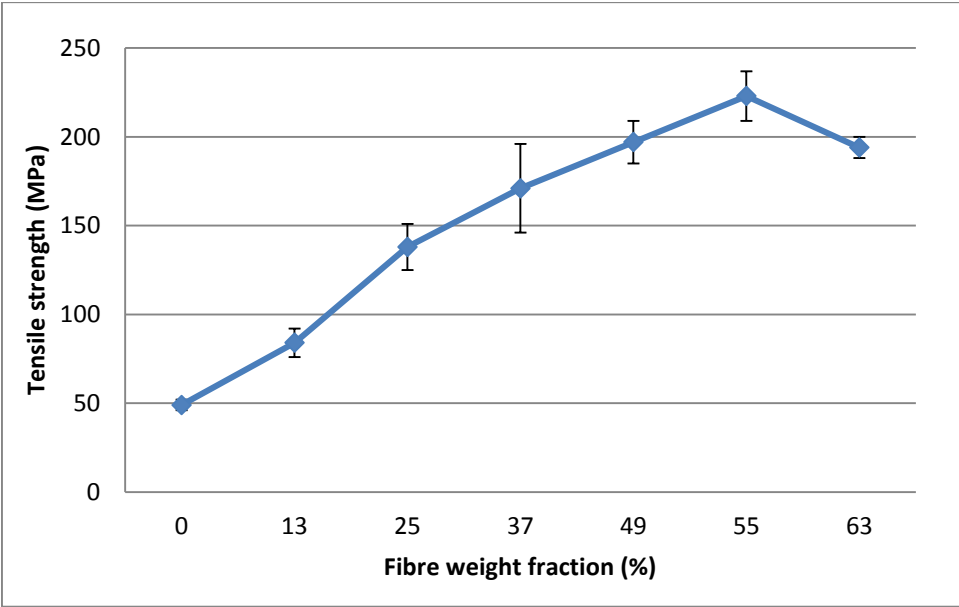


Fig. 8. Tensile strength of harekeke/epoxy composites versus fibre volume fraction; each error bar corresponds to one deviation.

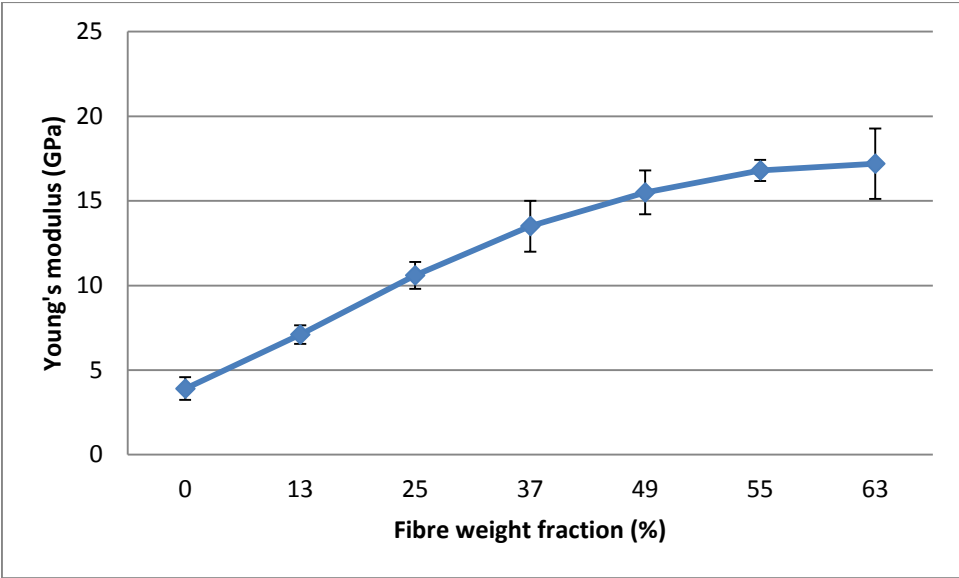


Fig. 9. Young's modulus of harekeke/epoxy composites versus fibre volume fraction; each error bar corresponds to one deviation.

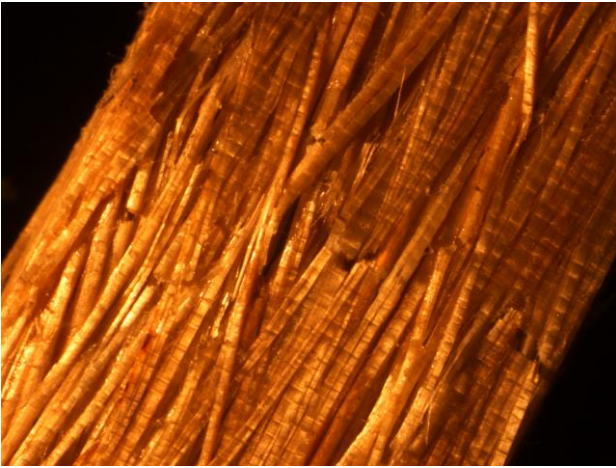


Fig. 10. Tension surface stereomicroscope micrograph of composites after flexural testing

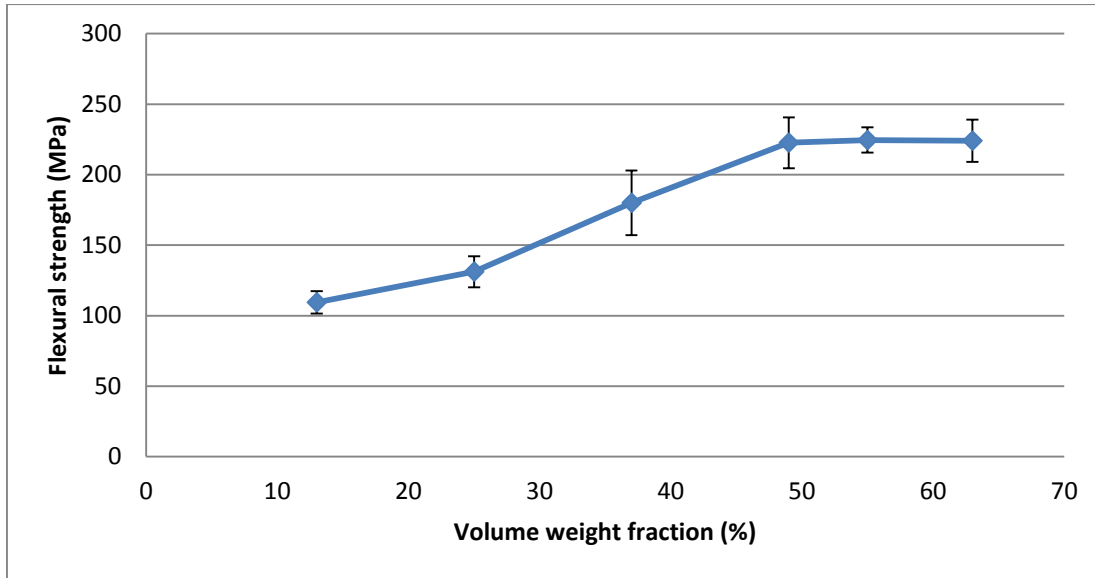


Fig. 11. Flexural strength of harakeke/epoxy composites versus fibre volume fraction; each error bar corresponds to one deviation.

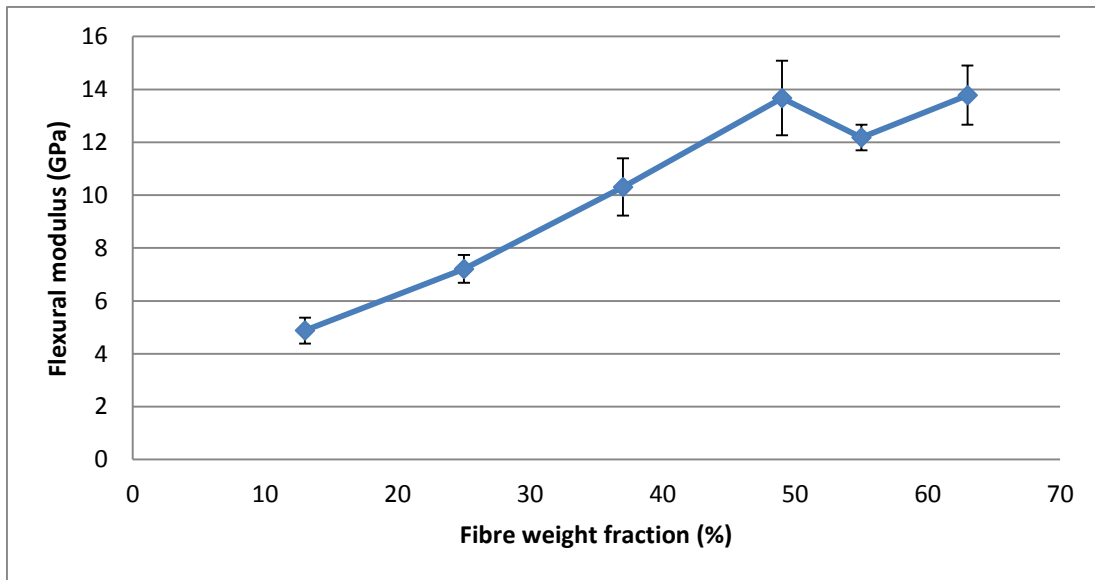


Fig. 12. Flexural modulus of harakeke/epoxy composites versus fibre volume fractions; each error bar corresponds to one deviation.

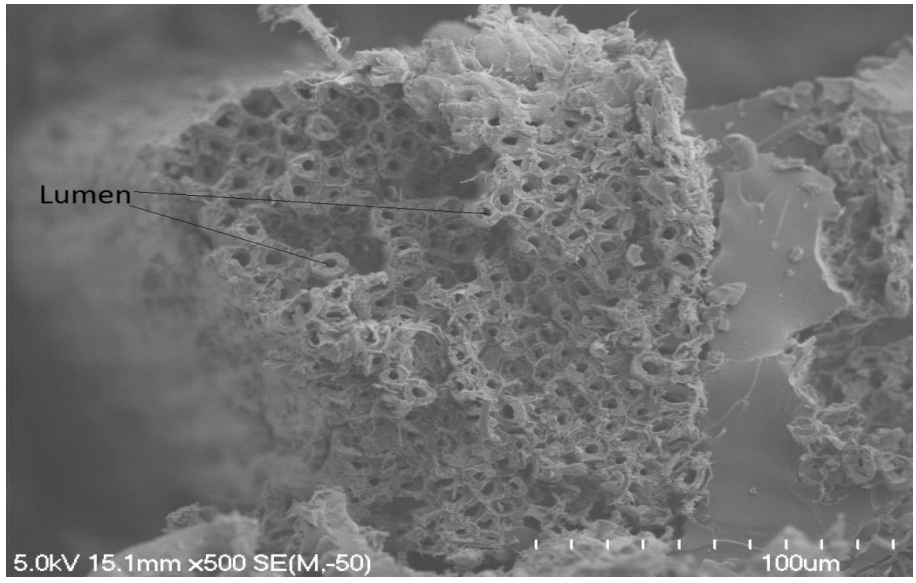


Fig. 13. FESEM arakeke fibre bundles in composites showing clear lumens

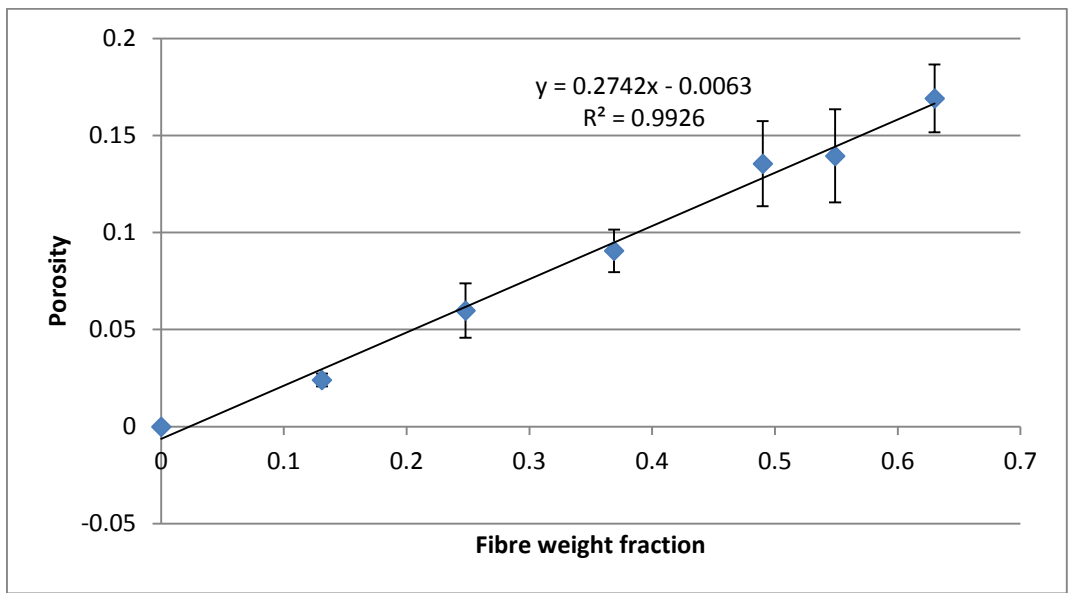


Fig. 14. Porosity modelling with linear equation; each error bar corresponds to one deviation.

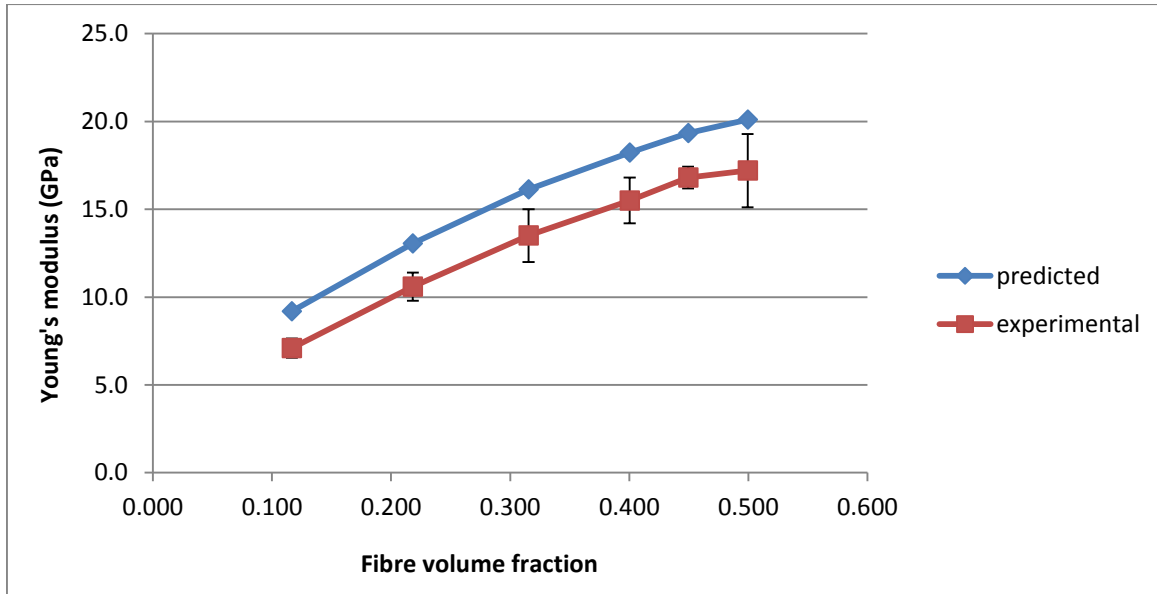


Fig. 15. Predicted Young's modulus (PYM) and experimental Young's modulus (EYM) of harakeke/epoxy composites as a function of fibre volume fraction; each error bar corresponds to one deviation.

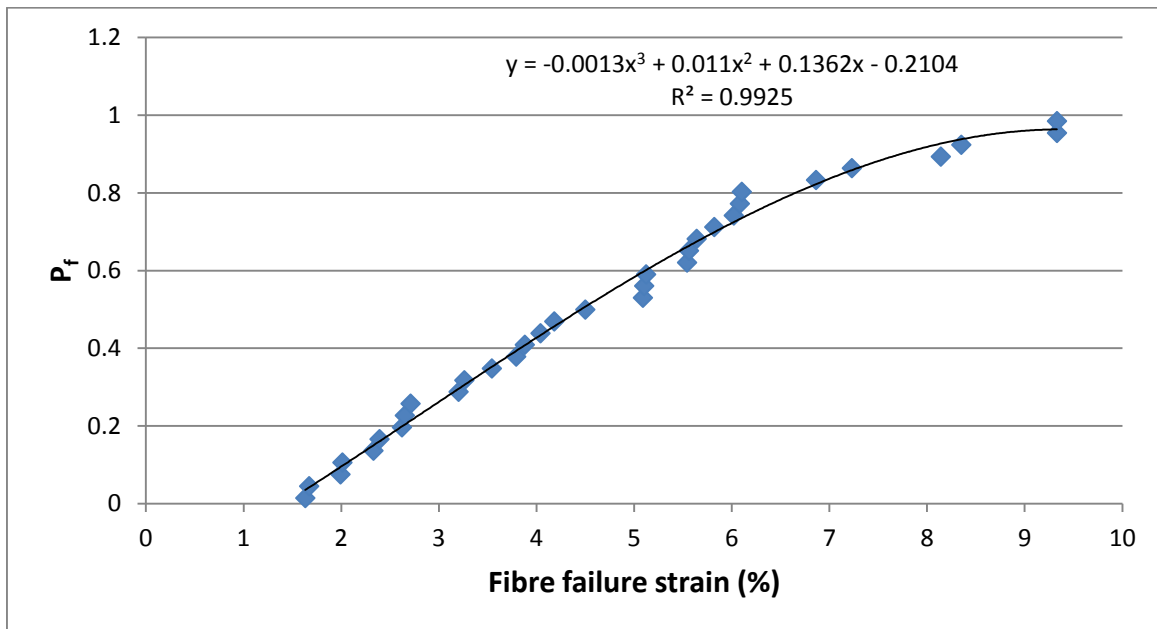


Fig. 16. Distribution of fibre failure strains

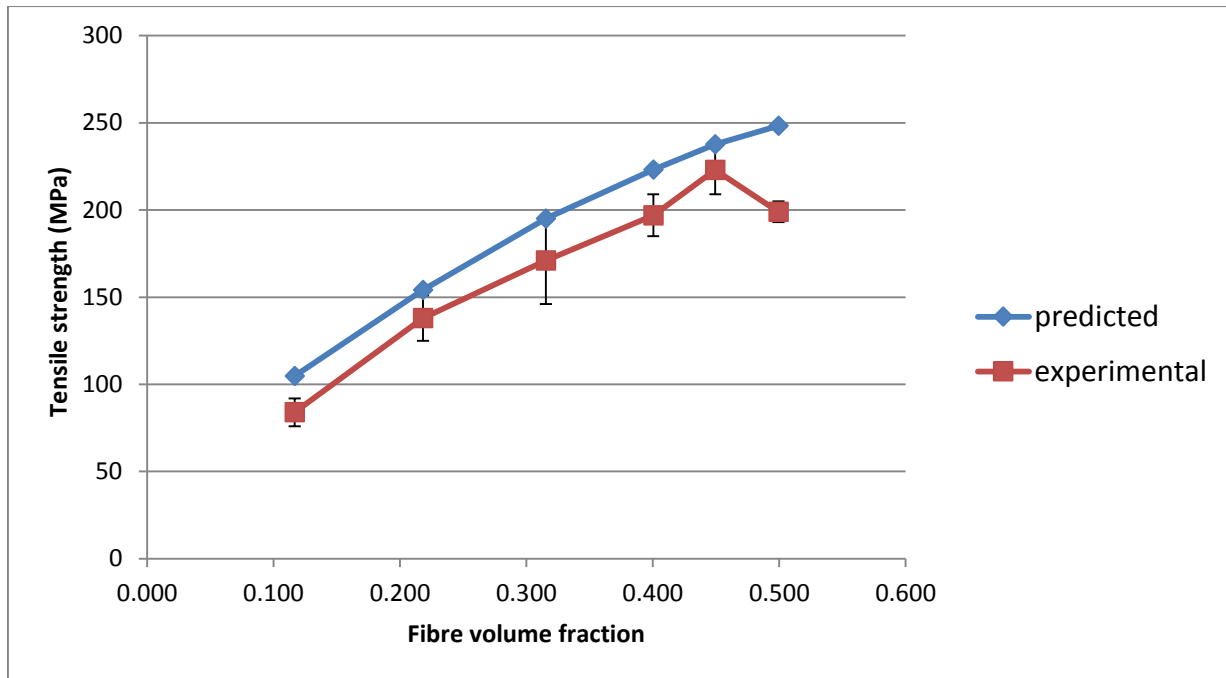


Fig. 17. Predicted strength (PS) and experimental strength (ES) of harakeke/epoxy composites as a function of fibre volume fraction (applying tensile stress of the fibre and matrix at strains of 1.41%); each error bar corresponds to one deviation.

Table 1: Comparison of lumen diameter, cell wall thickness and lumen fraction of various natural fibres.

Fibre	Flax [25]	Curaua [26]	Jute [26]	Sisal [26]	Harakeke
Lumen diameter (μm)	5	4	6.7	8.2	9.54
Cell wall thickness (μm)	-	3.5	2.5	2.6	2.72
Lumen fraction	0.068	0.041	0.254	0.252	0.214

Table 2: Comparison of harakeke fibre mechanical properties (standard deviation values in parenthesis) with other natural fibres.

Fibre	Density (g/cm^3)	Tensile strength (MPa)	Young's modulus (GPa)	Failure strain (%)	Ref
Harakeke	1.27	778	32.09	4.54	-

	(0.02)	(471)	(22.2)	(1.96)	
Sisal	1.45	468-640	9.4-22.0	3-7	[27]
Pineapple		413-1627	34.5-82.51	1.6	[27]
Flax	1.5	345-1100	27.6	2.7-3.2	[27]
Jute	1.3-1.45	393-773	13-26.5	1.16-1.5	[27]

Table 3: Comparison of harakeke composite tensile properties with glass and other natural fibre composites (standard deviation values in parenthesis).

Fibre	Matrix	Fibre content (%)	Density (g/cm ³)	Tensile strength (MPa)	Specific strength (MPa.g /cm ³)	Young's modulus (GPa)	Specific Young's modulus (GPa.g/cm ³)	Failure strain (%)	Ref
	Epoxy	0	1.16	49.2		3.91		2.91	-
Harakeke	Epoxy	55	1.04	223 (14)	214	16.8 (0.62)	16.2	1.44	-
Harakeke	Epoxy	50	1.16	211 (10)	181	14.7 (0.8)	12.6		[6]
Sisal	Epoxy	46		211 (12)	180	19.7 (1.5)	16.8		[28]
Hemp	Epoxy	65		165	-	17	-		[29]
Flax	Epoxy	40		133		28			[30]
Glass	Epoxy	48		817	487	31	18		[31]

Table 4: Physical properties of harakeke composites.

Fibre weight fraction	Composite density (g/cm ³)	Fibre volume fraction	Total porosity volume fraction	Lumen porosity volume fraction
0.131	1.143 (0.004)	0.118	0.025 (0.003)	0.025
0.248	1.112 (0.017)	0.216	0.060 (0.014)	0.046
0.369	1.086 (0.013)	0.315	0.091 (0.011)	0.067
0.490	1.041 (0.027)	0.400	0.135 (0.022)	0.086
0.549	1.041 (0.031)	0.449	0.139 (0.024)	0.096
0.630	1.010 (0.021)	0.499	0.169 (0.018)	0.107

Table 5: Comparison of predicted and experimental tensile strength of harakeke composites using average fibre and matrix tensile strength.

Fibre volume fraction	Predicted strength (MPa)	Experimental strength (MPa)	Prediction error (%)
0.117	197	84	135
0.218	326	138	136
0.315	449	171	163
0.400	557	197	183
0.449	619	223	178
0.499	683	199	243